

Supplementary Information

Routine monitoring of Western Lake Erie to track water quality changes associated with cyanobacterial harmful algal blooms

Authors:

Anna G Boegehold

Cooperative Institute for Great Lakes Research (CIGLR), University of Michigan, 4840 South State Road, Ann Arbor, MI 48108 USA

annaboeg@umich.edu

ORCID: 0000-0002-9718-9895

Ashley M. Burtner

Cooperative Institute for Great Lakes Research (CIGLR), University of Michigan, 4840 South State Road, Ann Arbor, MI 48108 USA

aburtner@umich.edu

Andrew C Camilleri

Cooperative Institute for Great Lakes Research (CIGLR), University of Michigan, 4840 South State Road, Ann Arbor, MI 48108 USA

accamill@umich.edu

Glenn Carter – CIGLR

Cooperative Institute for Great Lakes Research (CIGLR), University of Michigan, 4840 South State Road, Ann Arbor, MI 48108 USA

carterg@umich.edu

Paul DenUyl

Cooperative Institute for Great Lakes Research (CIGLR), University of Michigan, 4840 South State Road, Ann Arbor, MI 48108 USA

pdenuyl@umich.edu

ORCID: 0000-0003-3328-3476

David Fanslow

NOAA Great Lakes Environmental Research Laboratory, 4840 South State Road, Ann Arbor, MI 48108, USA

fanslowdl@gmail.com

Deanna Fyffe Semenyuk, Cooperative Institute for Great Lakes Research (CIGLR), University of Michigan, 4840 South State Road, Ann Arbor, MI 48108 and Jacobs, 1999 Bryan Street, Suite 1200, Dallas, TX, 75201, deanna.fyffe@jacobs.com

Casey M Godwin

Cooperative Institute for Great Lakes Research (CIGLR), University of Michigan, 4840 South State Road, Ann Arbor, MI 48108 USA

cgodwin@umich.edu

Duane Gossiaux

NOAA Great Lakes Environmental Research Laboratory, 4840 South State Road, Ann Arbor, MI 48108, USA

duane.gossiaux@noaa.gov

Thomas H Johengen

Cooperative Institute for Great Lakes Research (CI GLR), University of Michigan, 4840 South State Road, Ann Arbor, MI 48108 USA

johengen@umich.edu

Holly Kelchner

Cooperative Institute for Great Lakes Research (CI GLR), University of Michigan, 4840 South State Road, Ann Arbor, MI 48108 USA

hkelch@umich.edu

Christine Kitchens

Cooperative Institute for Great Lakes Research (CI GLR), University of Michigan, 4840 South State Road, Ann Arbor, MI 48108 USA

chknightl@umich.edu

ORCID: 0000-0002-8547-5704

Lacey A. Mason

NOAA Great Lakes Environmental Research Laboratory, 4840 South State Road, Ann Arbor, MI 48108 USA

lacey.mason@noaa.gov

ORCID: 0000-0003-1541-3134

Kelly McCabe

Cooperative Institute for Great Lakes Research (CI GLR), University of Michigan, 4840 South State Road, Ann Arbor, MI 48108 USA

mccabekm@umich.edu

Danna Palladino

NOAA Great Lakes Environmental Research Laboratory, 4840 South State Road, Ann Arbor, MI 48108

danna.palladino@noaa.gov

ORCID: 0000-0003-4840-3493

Dack Stuart

Woods Hole Group, Inc., 107 Waterhouse Road, Bourne, MA 02532,

dstuart@woodsholegroup.com

ORCID: 0000-0002-3796-081X

Henry Vanderploeg

NOAA Great Lakes Environmental Research Laboratory, 4840 South State Road, Ann Arbor, MI 48108

henry.vanderploeg@noaa.gov

ORCID: 0000-0003-1358-8475

Reagan Errera

NOAA Great Lakes Environmental Research Laboratory, 4840 South State Road, Ann Arbor, MI 48108, USA

reagan.errera@noaa.gov

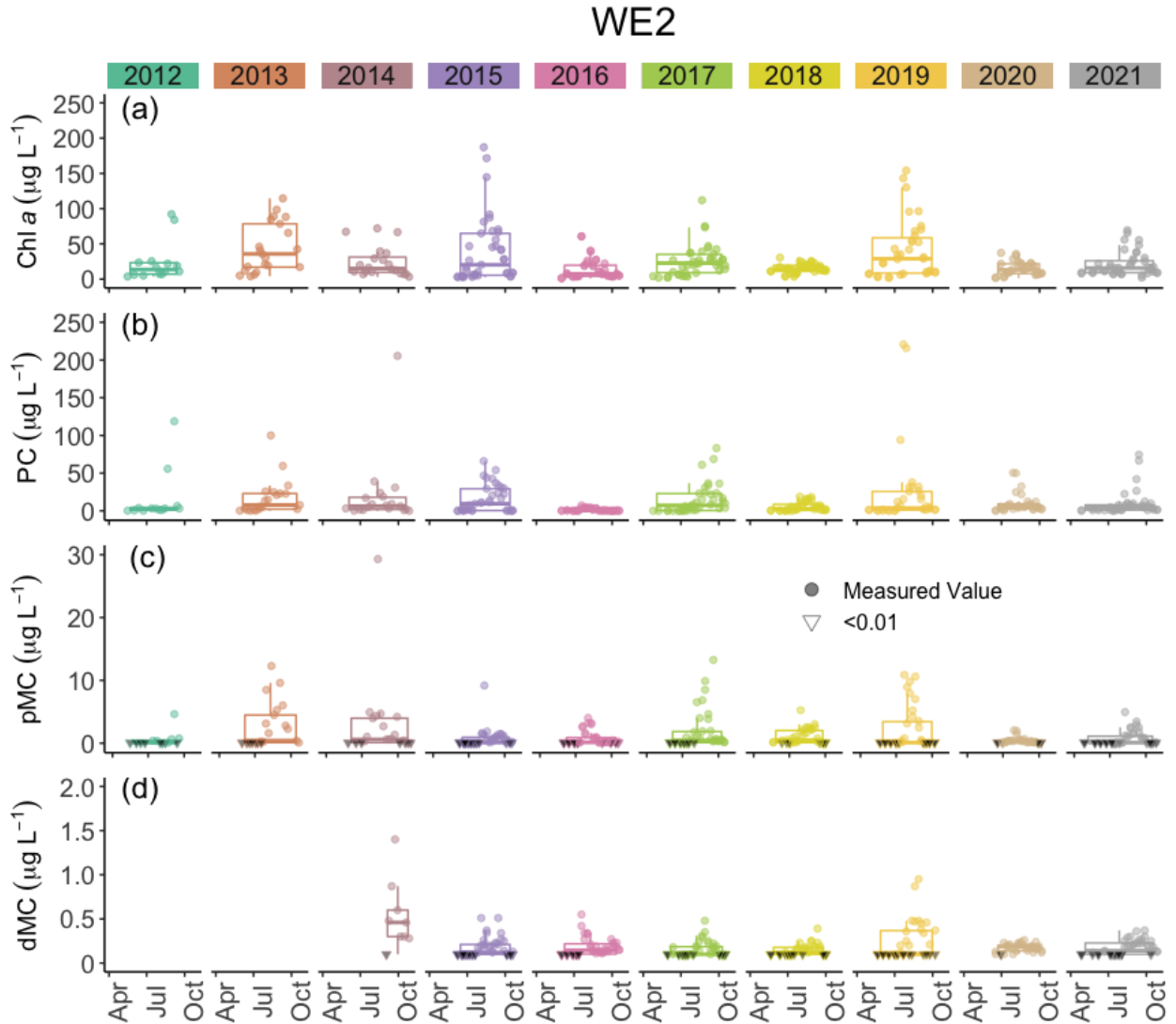


Figure S1. Concentrations of chlorophyll *a* (Chl *a*), phycocyanin (PC), particulate microcystins (pMC), and dissolved microcystins (dMC) at Station WE02 for all years sampled. Boxplots represent the median and 25% and 75% quartiles with whiskers extending to the highest or lowest point within 1.5x the interquartile range. A scatterplot is overlaid on the boxplots.

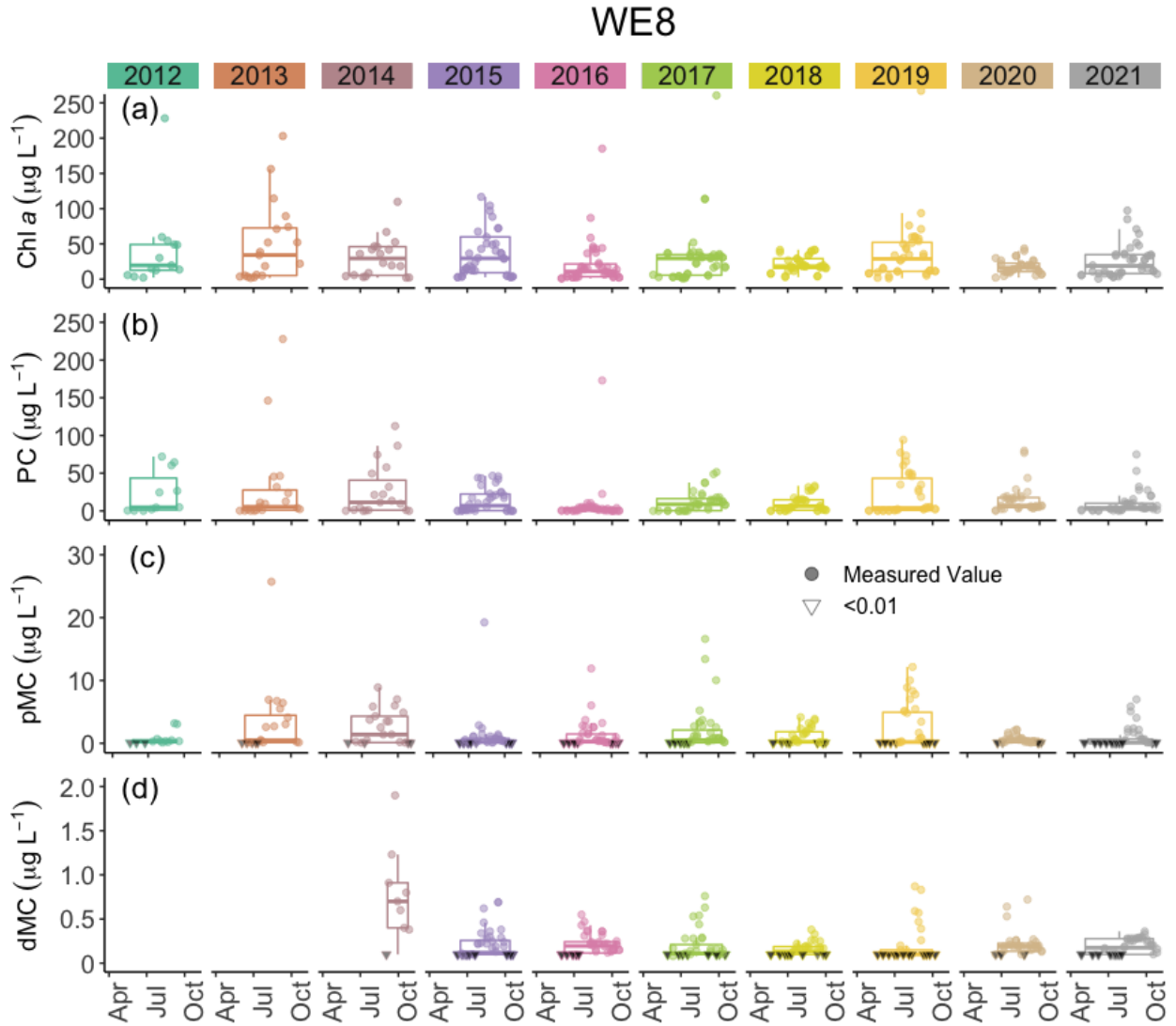


Figure S2. Concentrations of chlorophyll a (Chl a), phycocyanin (PC), particulate microcystins (pMC), and dissolved microcystins (dMC) at Station WE08 for all years sampled. Boxplots represent the median and 25% and 75% quartiles with whiskers extending to the highest or lowest point within 1.5x the interquartile range. A scatterplot is overlaid on the boxplots.

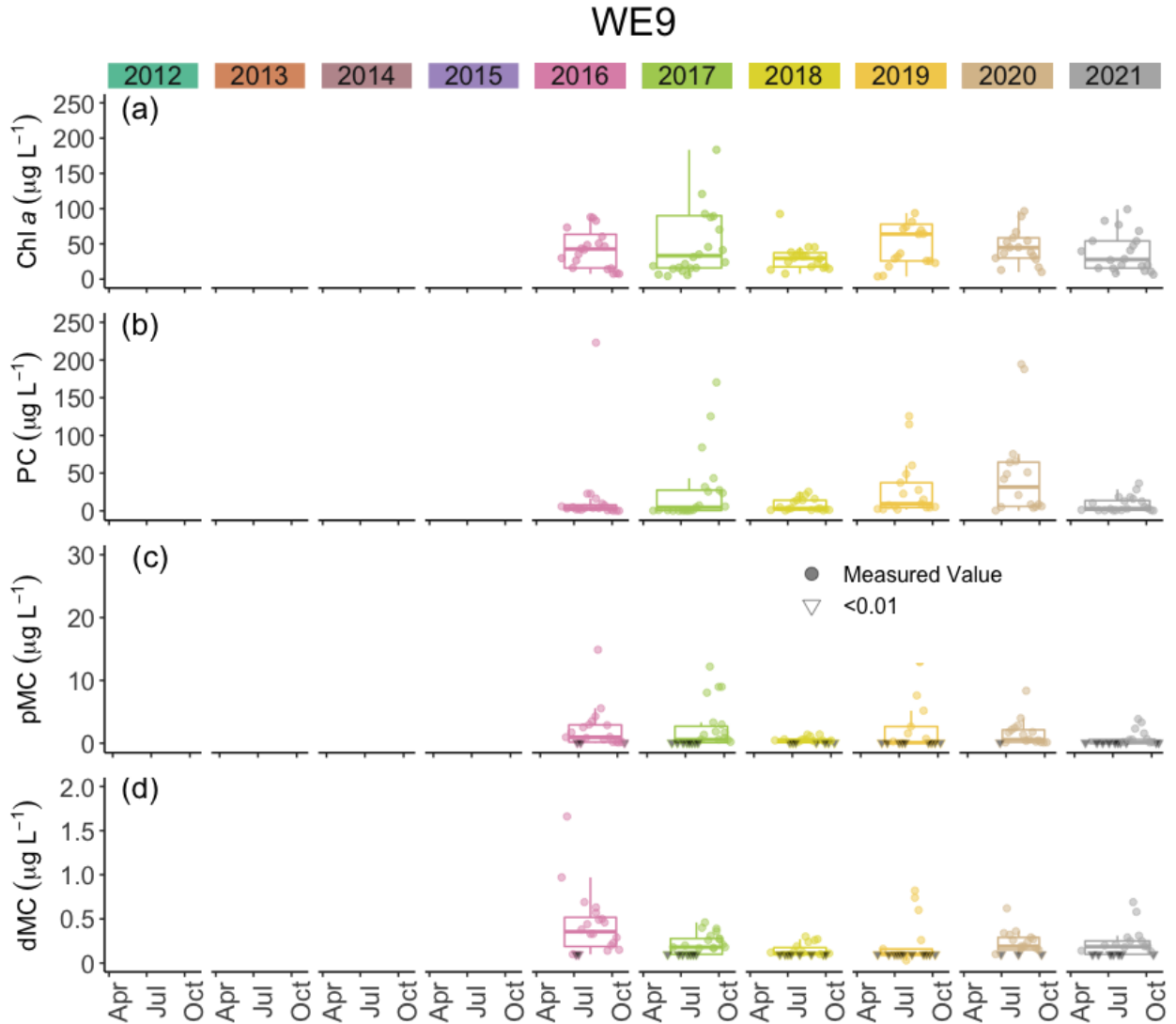


Figure S3. Concentrations of chlorophyll a (Chl a), phycocyanin (PC), particulate microcystins (pMC), and dissolved microcystins (dMC) at Station WE09 for all years sampled. Boxplots represent the median and 25% and 75% quartiles with whiskers extending to the highest or lowest point within 1.5x the interquartile range. A scatterplot is overlaid on the boxplots.

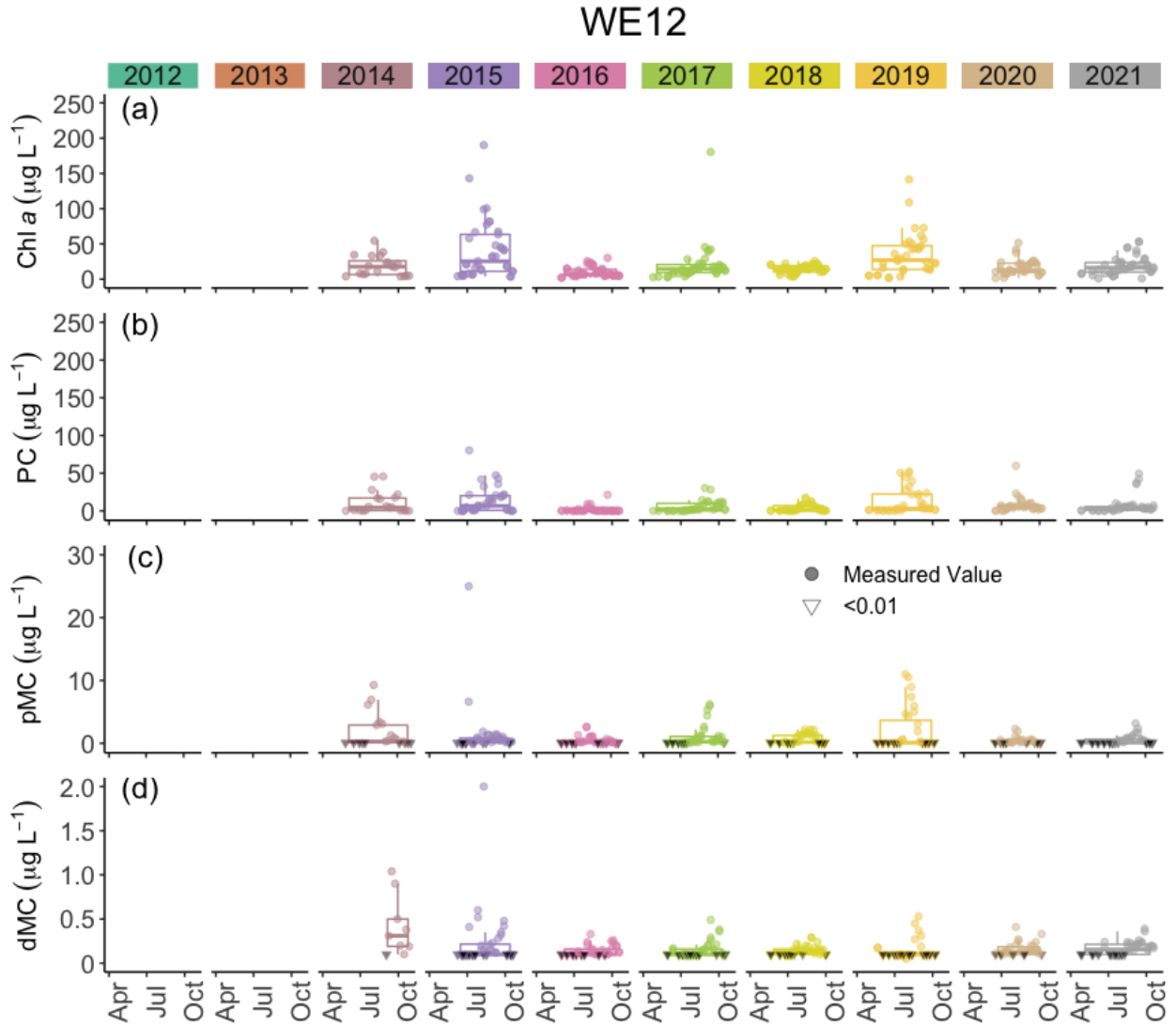


Figure S4. Concentrations of chlorophyll a (Chl a), phycocyanin (PC), particulate microcystins (pMC), and dissolved microcystins (dMC) at Station WE12 for all years sampled. Boxplots represent the median and 25% and 75% quartiles with whiskers extending to the highest or lowest point within 1.5x the interquartile range. A scatterplot is overlaid on the boxplots.

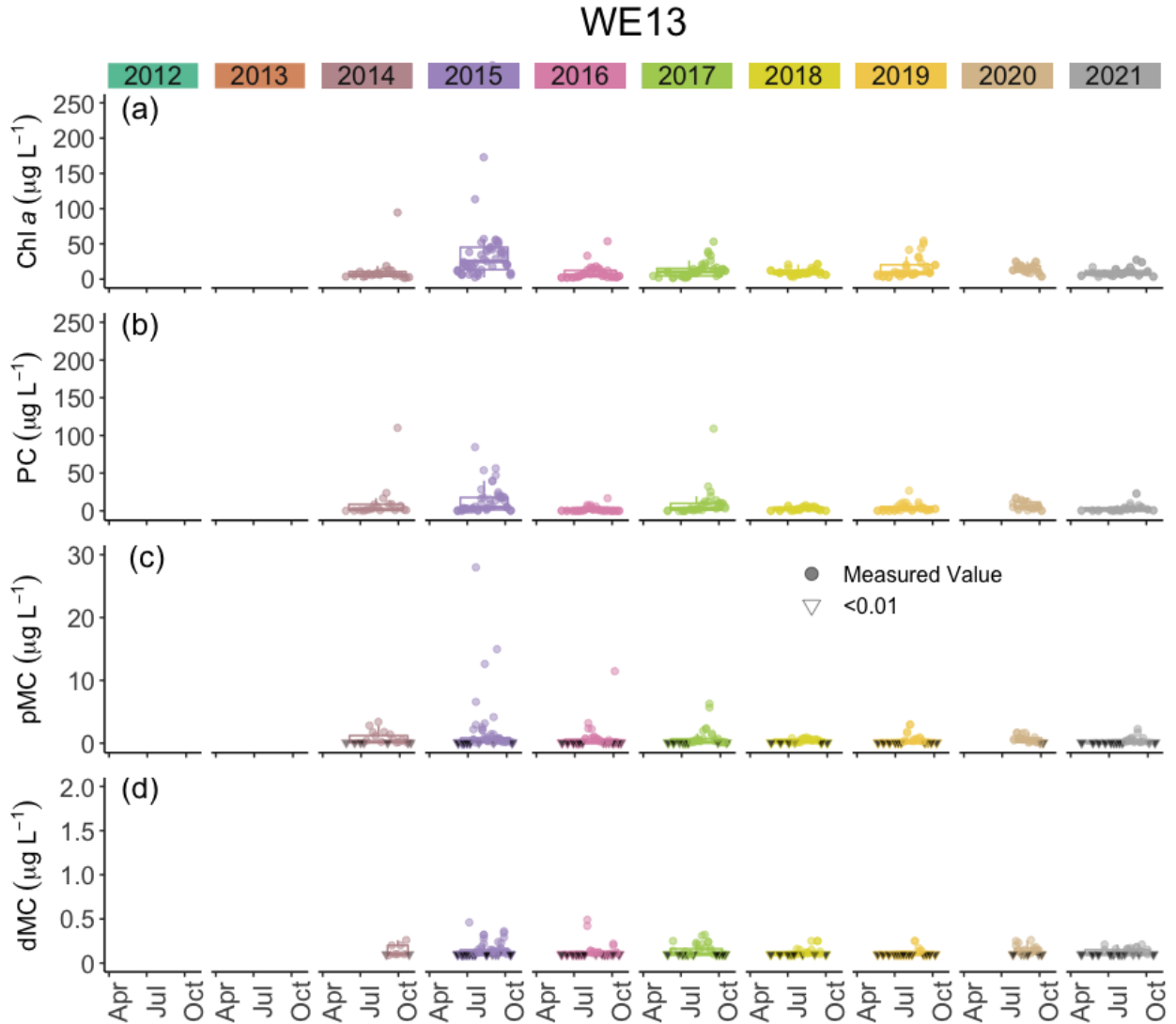


Figure S5. Concentrations of chlorophyll a (Chl a), phycocyanin (PC), particulate microcystins (pMC), and dissolved microcystins (dMC) at Station WE13 for all years sampled. Boxplots represent the median and 25% and 75% quartiles with whiskers extending to the highest or lowest point within 1.5x the interquartile range. A scatterplot is overlaid on the boxplots.

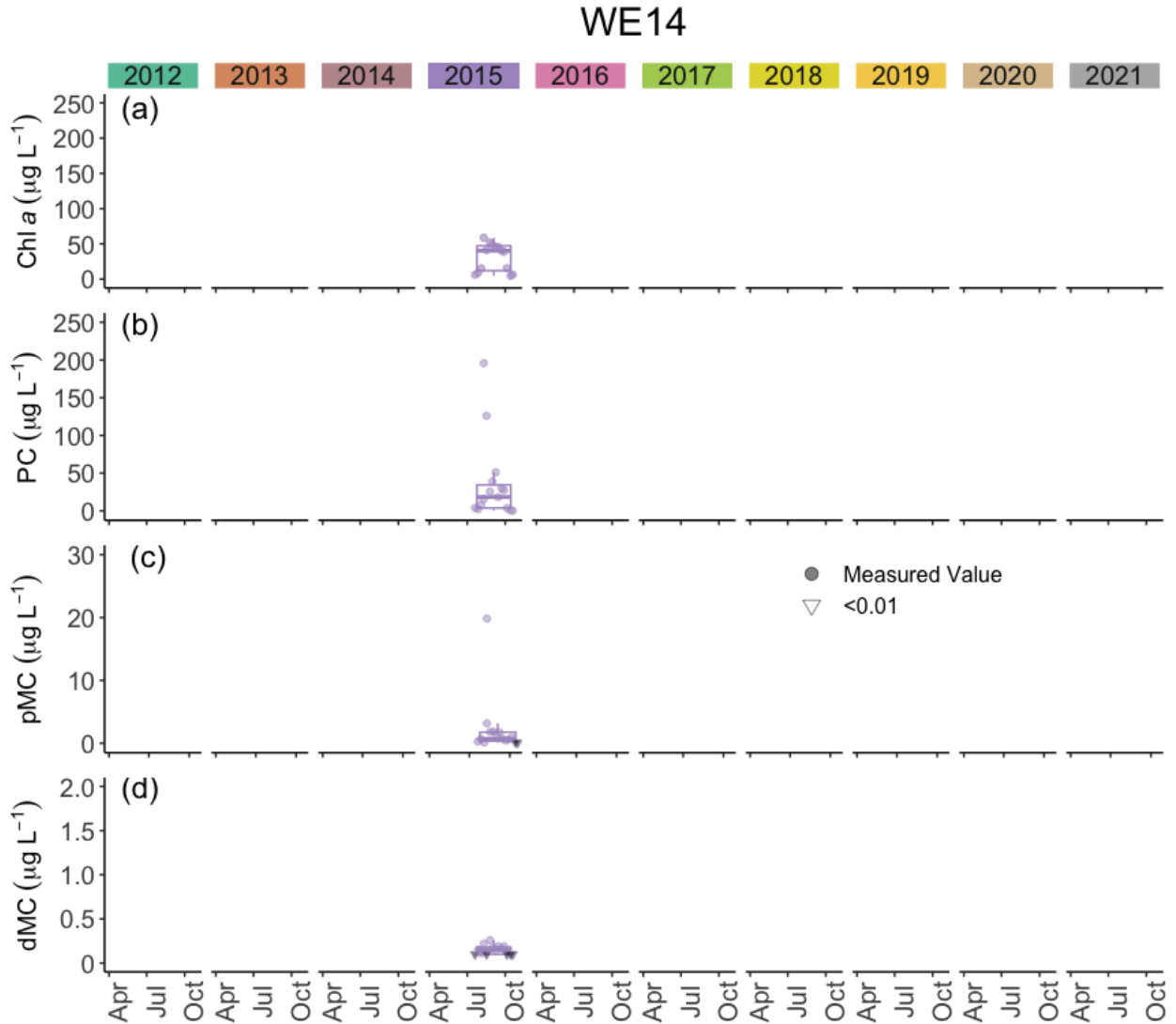


Figure S6. Concentrations of chlorophyll a (Chl a), phycocyanin (PC), particulate microcystins (pMC), and dissolved microcystins (dMC) at Station WE14 for all years sampled. Boxplots represent the median and 25% and 75% quartiles with whiskers extending to the highest or lowest point within 1.5x the interquartile range. A scatterplot is overlaid on the boxplots.

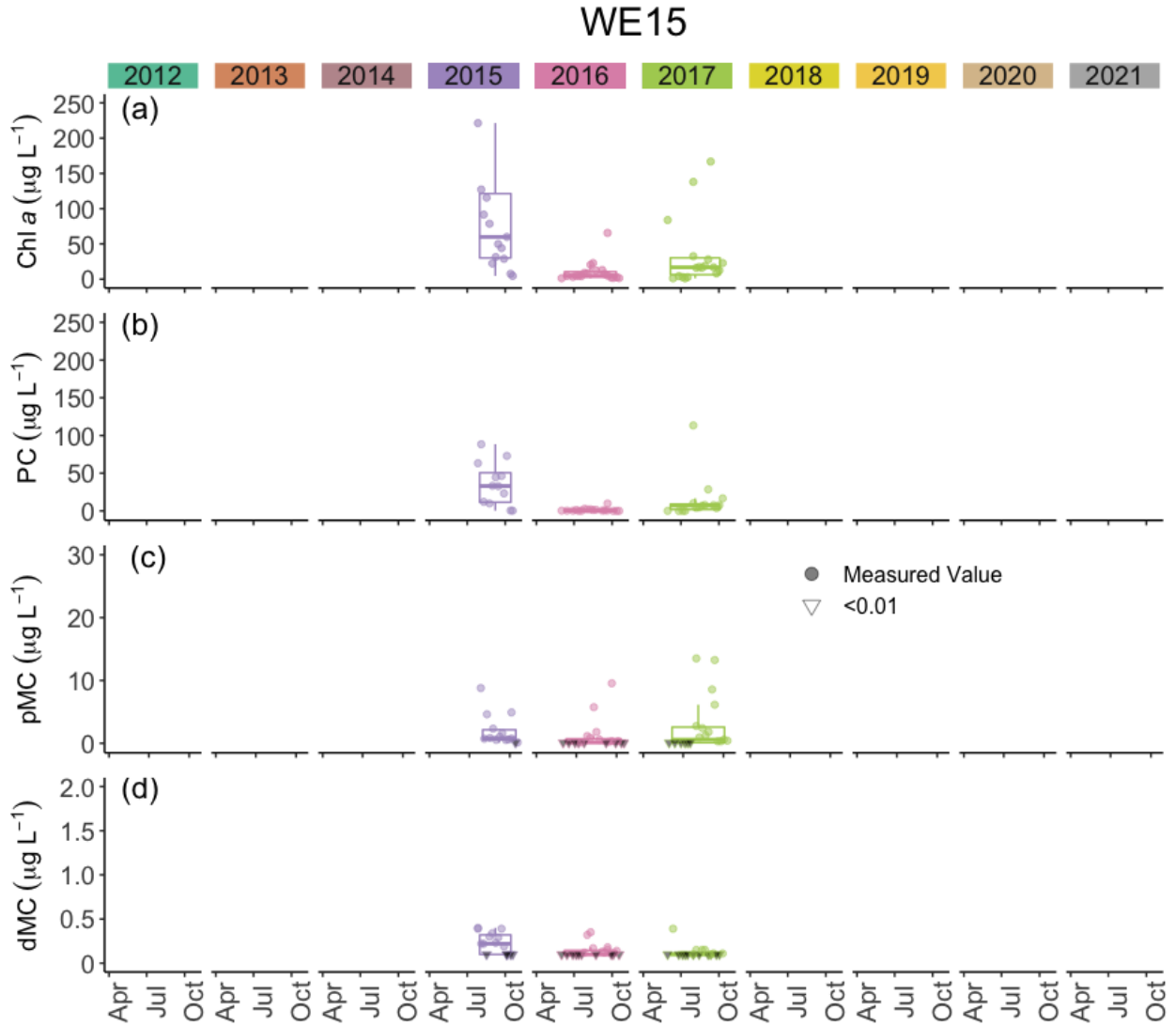


Figure S7. Concentrations of chlorophyll a (Chl a), phycocyanin (PC), particulate microcystins (pMC), and dissolved microcystins (dMC) at Station WE15 for all years sampled. Boxplots represent the median and 25% and 75% quartiles with whiskers extending to the highest or lowest point within 1.5x the interquartile range. A scatterplot is overlaid on the boxplots.

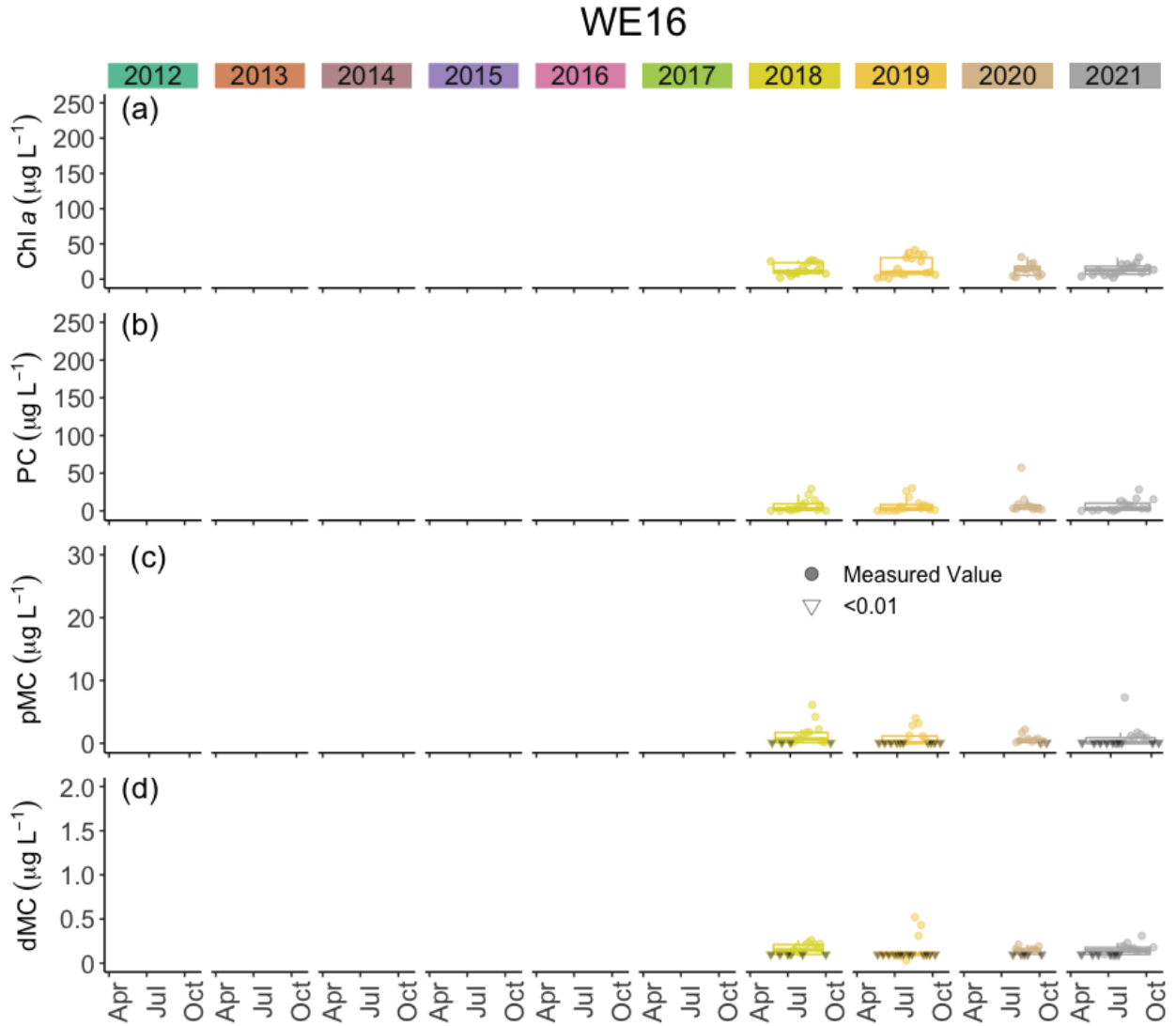


Figure S8. Concentrations of chlorophyll a (Chl a), phycocyanin (PC), particulate microcystins (pMC), and dissolved microcystins (dMC) at Station WE16 for all years sampled. Boxplots represent the median and 25% and 75% quartiles with whiskers extending to the highest or lowest point within 1.5x the interquartile range. A scatterplot is overlaid on the boxplots.

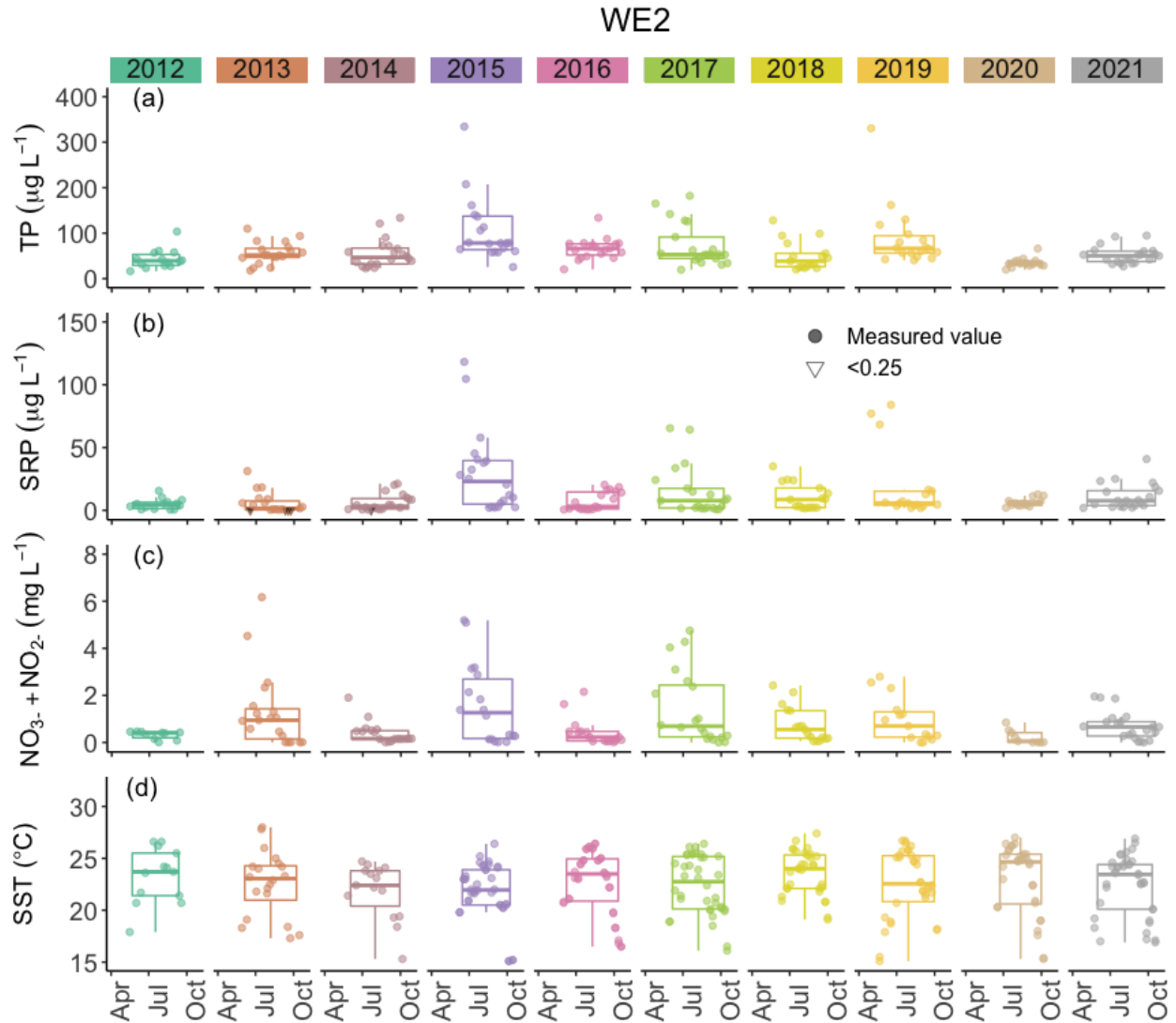


Figure S9. Concentrations of total phosphorus (TP), soluble reactive phosphorus (SRP), nitrate plus nitrite ($\text{NO}_3^- + \text{NO}_2^-$), and sea surface temperature (SST) at Station WE02 for all years sampled. Boxplots represent the median and 25% and 75% quartiles with whiskers extending to the highest or lowest point within 1.5x the interquartile range. A scatterplot is overlaid on the boxplots.

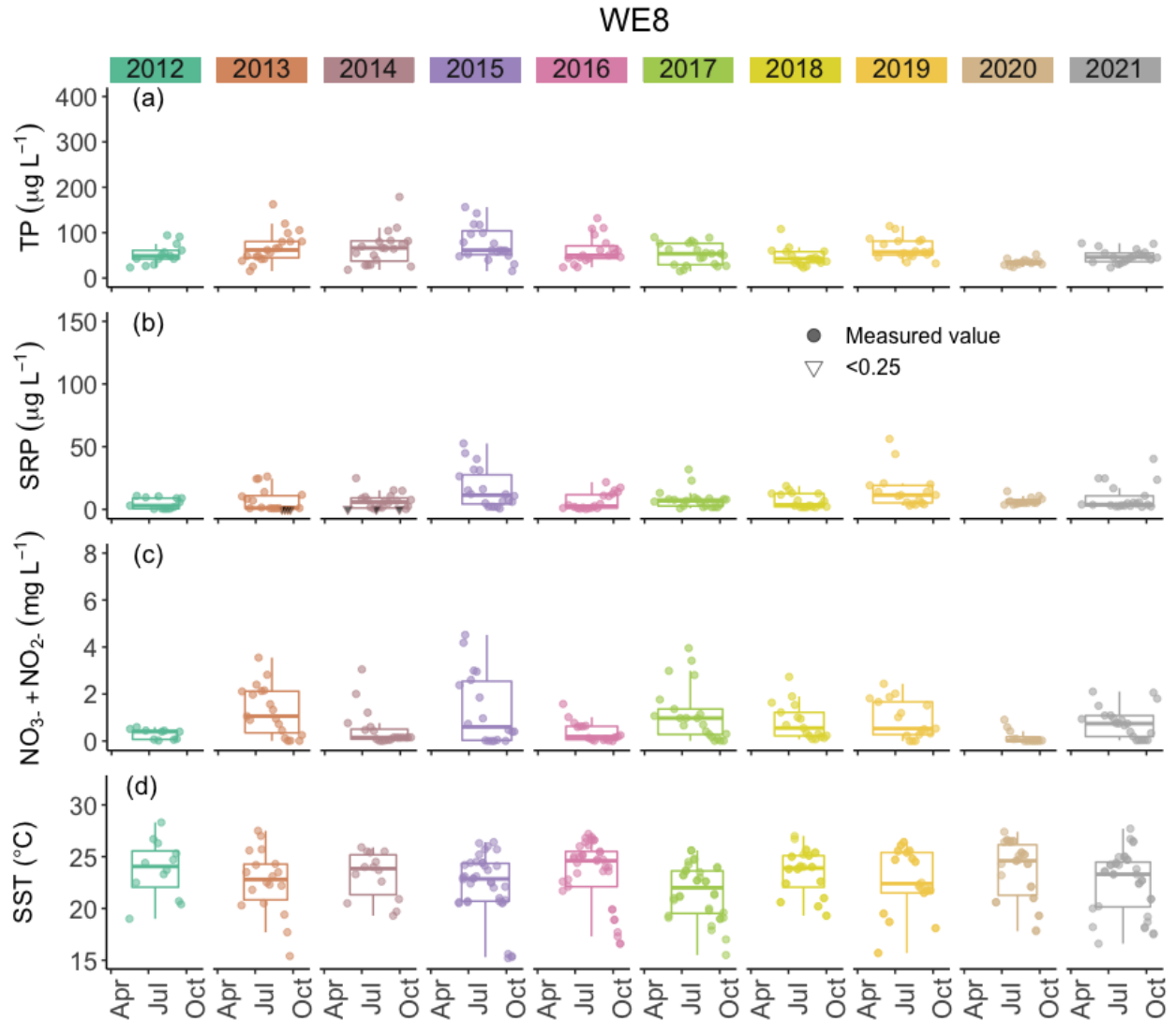


Figure S10. Concentrations of total phosphorus (TP), soluble reactive phosphorus (SRP), nitrate plus nitrite ($\text{NO}_3^- + \text{NO}_2^-$), and sea surface temperature (SST) at Station WE08 for all years sampled. Boxplots represent the median and 25% and 75% quartiles with whiskers extending to the highest or lowest point within 1.5x the interquartile range. A scatterplot is overlaid on the boxplots.

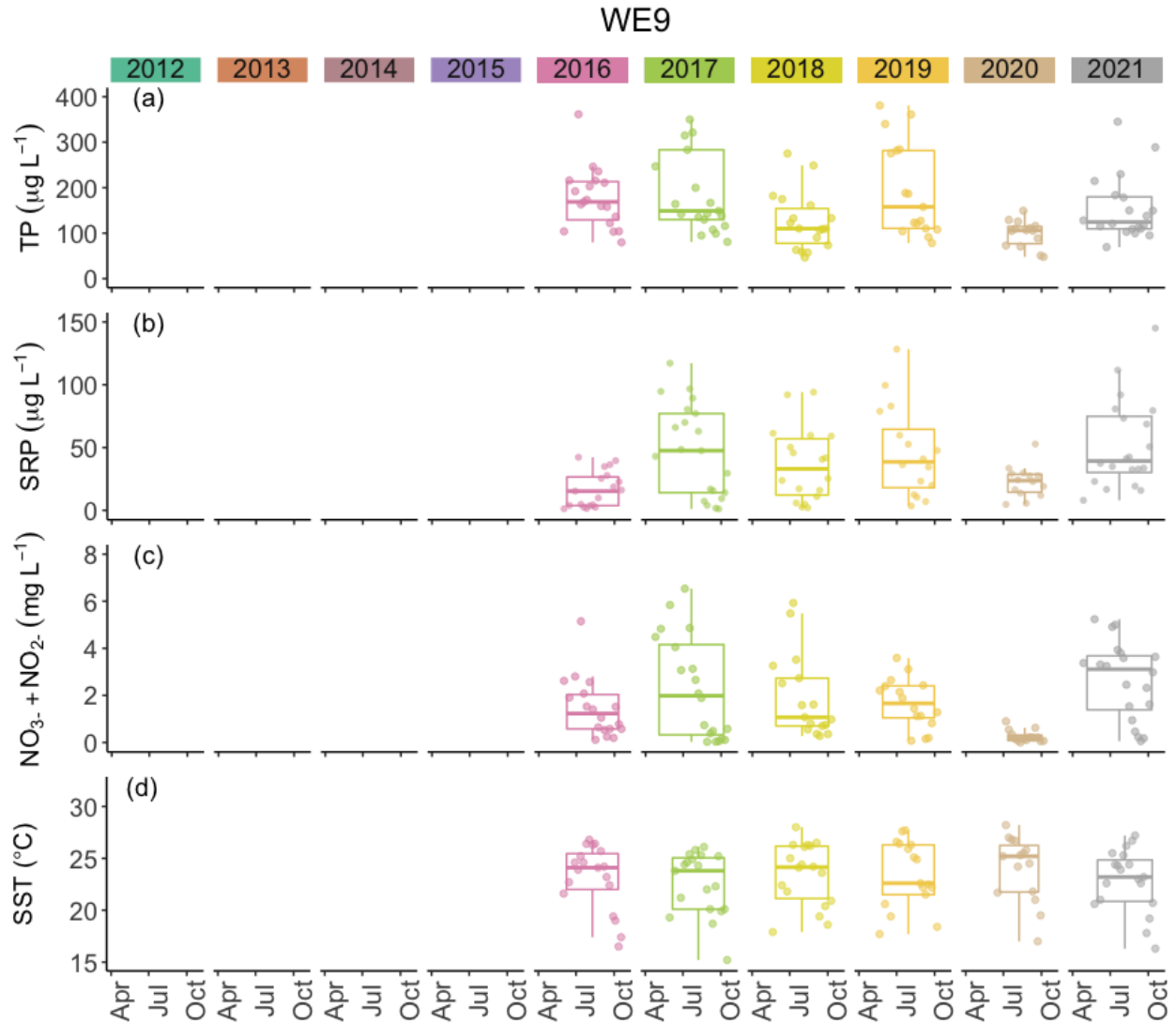


Figure S11. Concentrations of total phosphorus (TP), soluble reactive phosphorus (SRP), nitrate plus nitrite ($\text{NO}_3^- + \text{NO}_2^-$), and sea surface temperature (SST) at Station WE09 for all years sampled. Boxplots represent the median and 25% and 75% quartiles with whiskers extending to the highest or lowest point within 1.5x the interquartile range. A scatterplot is overlaid on the boxplots.

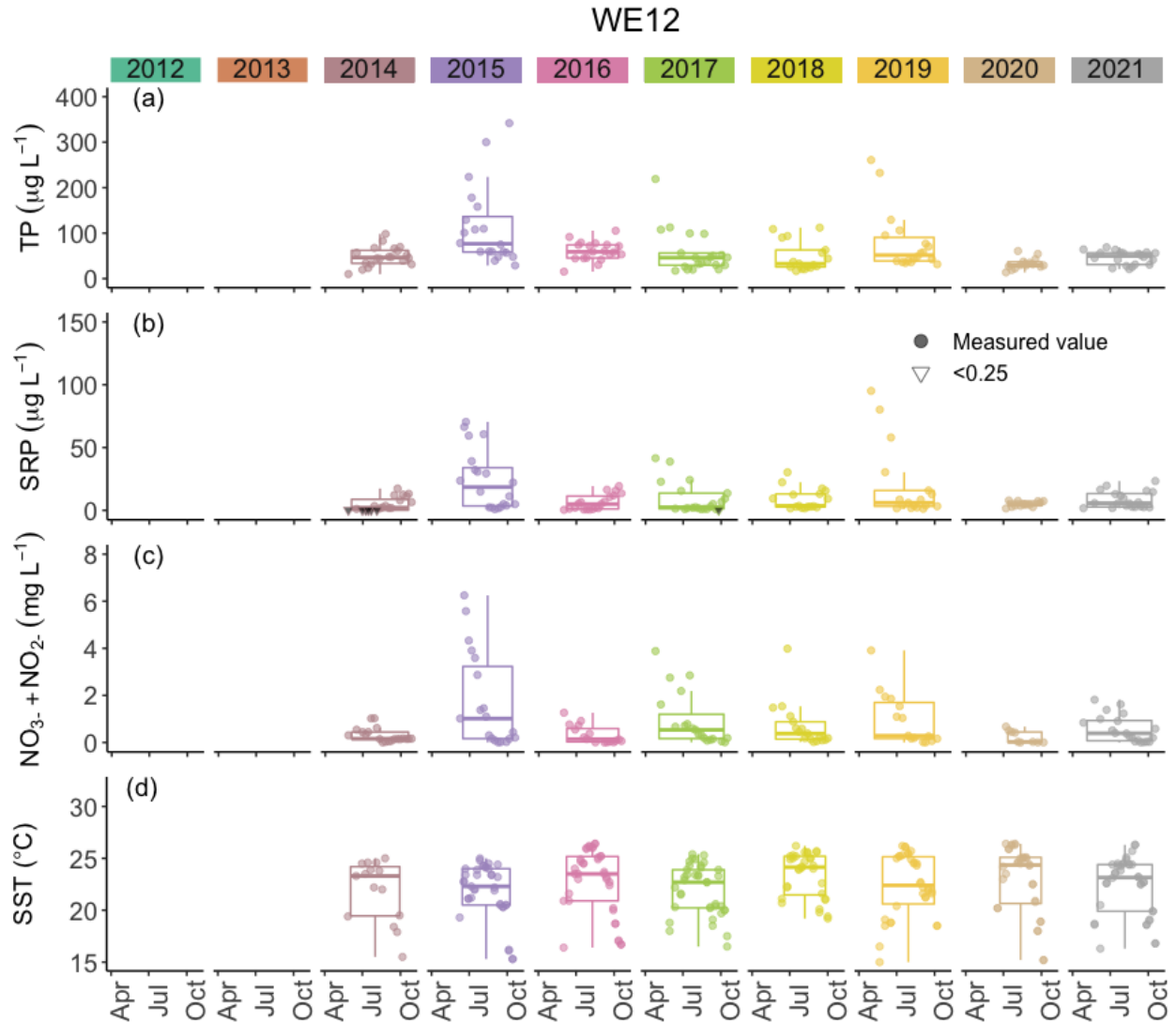


Figure S12. Concentrations of total phosphorus (TP), soluble reactive phosphorus (SRP), nitrate plus nitrite ($\text{NO}_3^- + \text{NO}_2^-$), and sea surface temperature (SST) at Station WE12 for all years sampled. Boxplots represent the median and 25% and 75% quartiles with whiskers extending to the highest or lowest point within 1.5x the interquartile range. A scatterplot is overlaid on the boxplots.

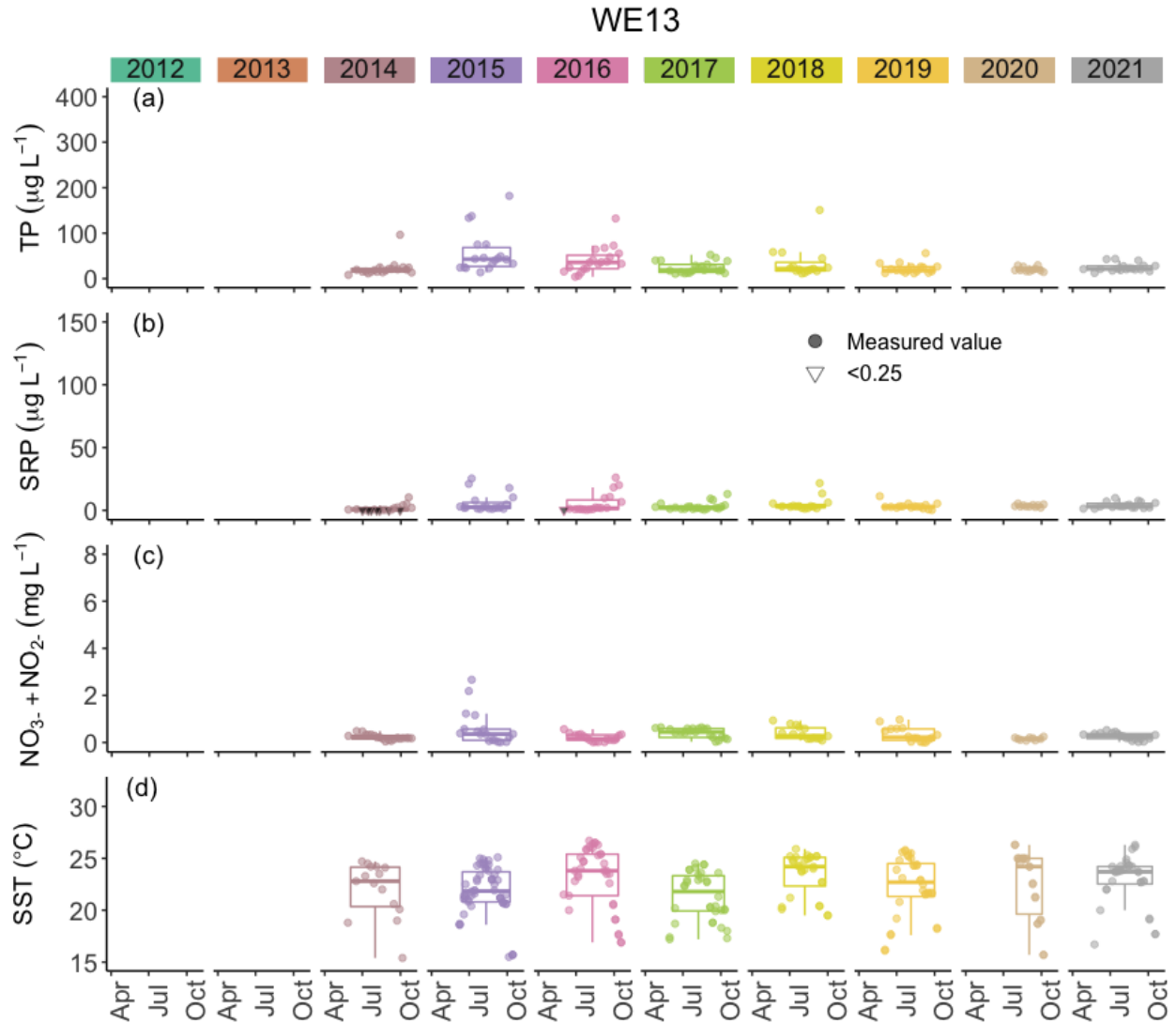


Figure S13. Concentrations of total phosphorus (TP), soluble reactive phosphorus (SRP), nitrate plus nitrite ($\text{NO}_3^- + \text{NO}_2^-$), and sea surface temperature (SST) at Station WE13 for all years sampled. Boxplots represent the median and 25% and 75% quartiles with whiskers extending to the highest or lowest point within 1.5x the interquartile range. A scatterplot is overlaid on the boxplots.

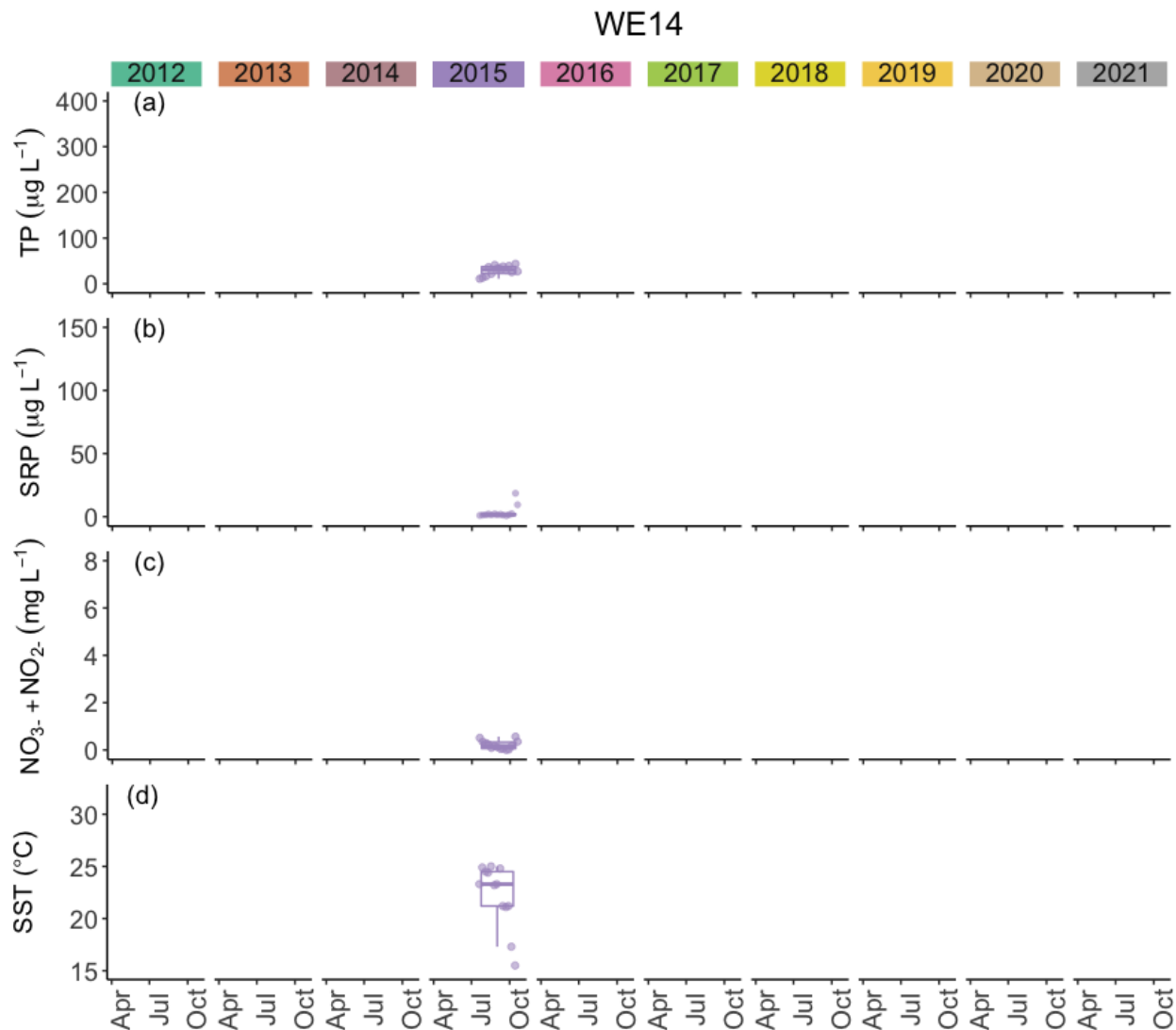


Figure S14. Concentrations of total phosphorus (TP), soluble reactive phosphorus (SRP), nitrate plus nitrite ($\text{NO}_3^- + \text{NO}_2^-$), and sea surface temperature (SST) at Station WE14 for all years sampled. Boxplots represent the median and 25% and 75% quartiles with whiskers extending to the highest or lowest point within 1.5x the interquartile range. A scatterplot is overlaid on the boxplots.

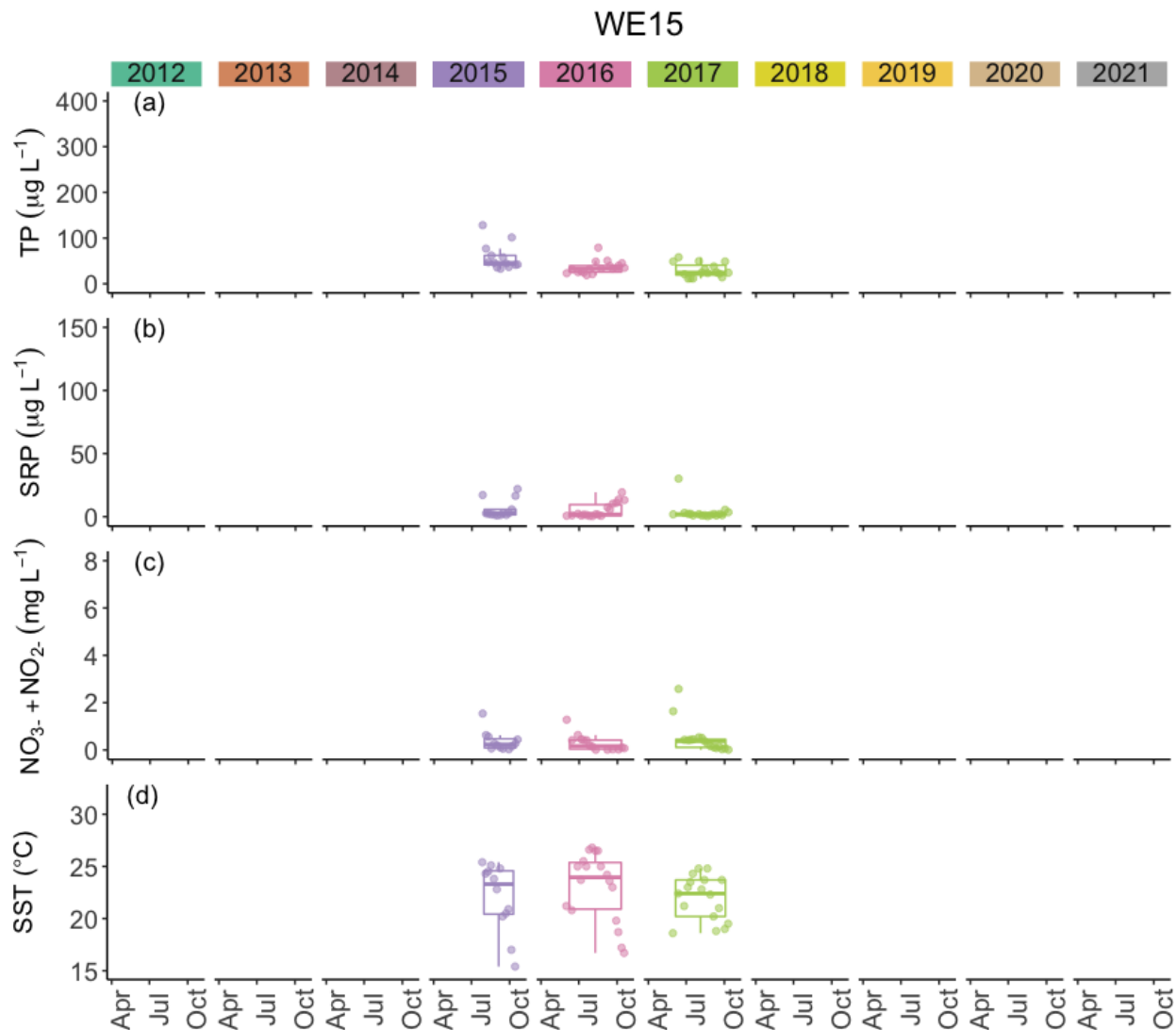


Figure S15. Concentrations of total phosphorus (TP), soluble reactive phosphorus (SRP), nitrate plus nitrite ($\text{NO}_3^- + \text{NO}_2^-$), and sea surface temperature (SST) at Station WE15 for all years sampled. Boxplots represent the median and 25% and 75% quartiles with whiskers extending to the highest or lowest point within 1.5x the interquartile range. A scatterplot is overlaid on the boxplots.

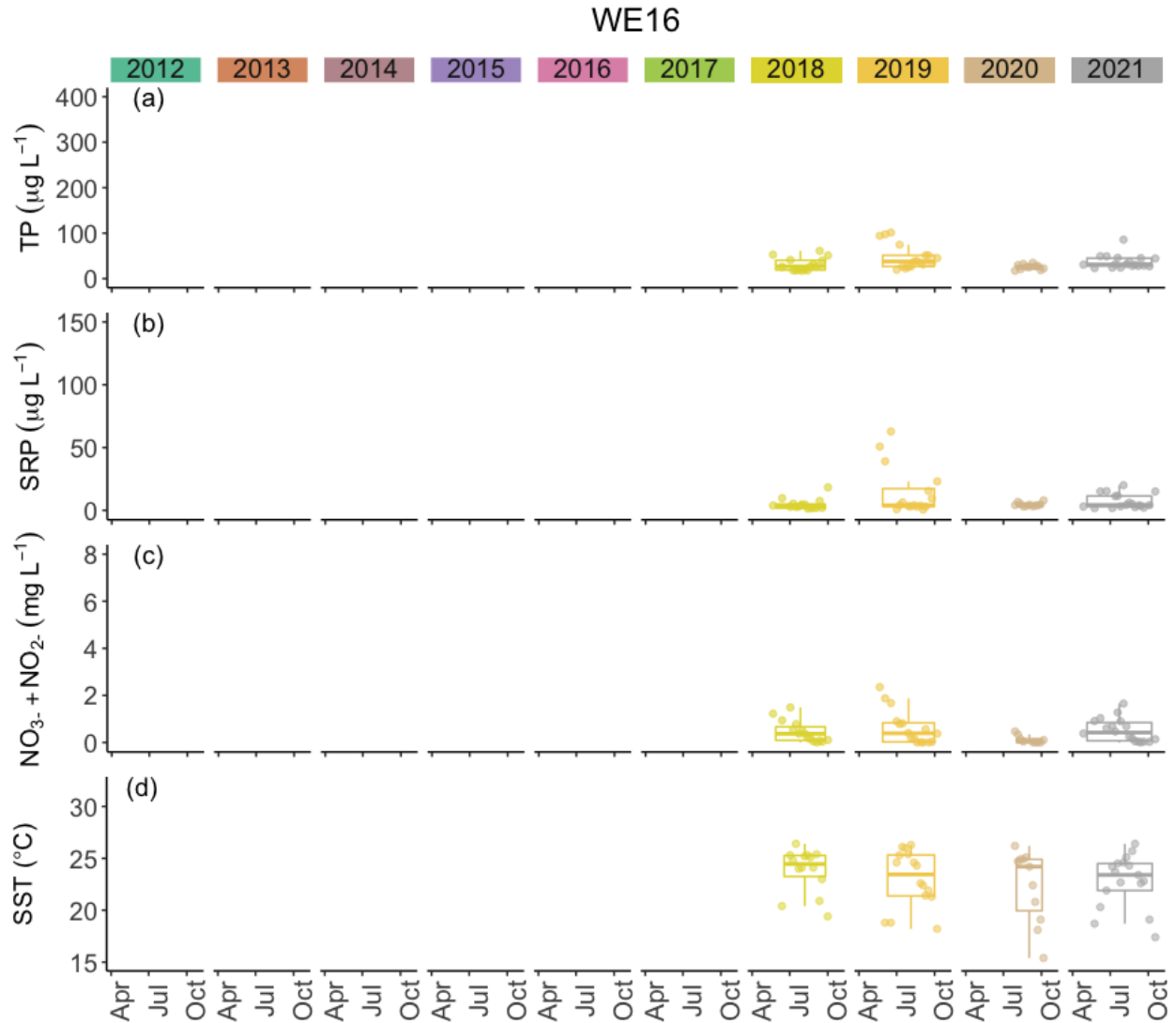


Figure S16. Concentrations of total phosphorus (TP), soluble reactive phosphorus (SRP), nitrate plus nitrite ($\text{NO}_3^- + \text{NO}_2^-$), and sea surface temperature (SST) at Station WE16 for all years sampled. Boxplots represent the median and 25% and 75% quartiles with whiskers extending to the highest or lowest point within 1.5x the interquartile range. A scatterplot is overlaid on the boxplots.